Earth and Planetary Science Letters 308 (2011) 410–416

Contents lists available at ScienceDirect

Earth and Planetary Science Letters

journal homepage: www.elsevier.com/locate/epsl

# Size of the group IVA iron meteorite core: Constraints from the age and composition of Muonionalusta

Nicholas A. Moskovitz [a,*], Richard J. Walker [b]

[a] Carnegie Institution of Washington, Department of Terrestrial Magnetism, 5241 Broad Branch Road, Washington, DC 20015, USA
[b] University of Maryland, Department of Geology, College Park, MD 20742, USA

ARTICLE INFO

*Article history:*
Received 10 December 2010
Received in revised form 6 June 2011
Accepted 11 June 2011
Available online 30 June 2011

Editor: T. Spohn

*Keywords:*
iron meteorites
planetary differentiation
early Solar System

ABSTRACT

The group IVA fractionally crystallized iron meteorites display a diverse range of metallographic cooling rates. These have been attributed to their formation in a metallic core, approximately 150 km in radius, that cooled to crystallization in the absence of any appreciable insulating mantle. Here we build upon this formation model by incorporating several new constraints. These include (i) a recent U–Pb radiometric closure age of <2.5 Myr after solar system formation for the group IVA iron Muonionalusta, (ii) new measurements and modeling of highly siderophile element compositions for a suite of IVAs, and (iii) consideration of the thermal effects of heating by the decay of the short-lived radionuclide $^{60}$Fe. Our model for the thermal evolution of the IVA core suggests that it was approximately 50–110 km in radius after being collisionally exposed. This range is due to uncertainties in the initial abundance of live $^{60}$Fe incorporated into the IVA core. Our models define a relationship between cooling rate and closure age, which is used to make several predictions that can be tested with future measurements. In general, our results show that diverse cooling rates and early U–Pb closure ages can only coexist on mantle-free bodies and that energy released by the decay of $^{60}$Fe reduces the core size necessary to produce diverse metallographic cooling rates. The influence of $^{60}$Fe on cooling rates has largely been neglected in previous core formation models; accounting for this heat source can affect size estimates for other iron meteorite cores that cooled to crystallization in the presence of live $^{60}$Fe. Candidates for such a scenario of early, mantle-free formation include the iron IIAB, IIIAB and IVB groups.



## 1. Introduction

Amongst the oldest melted rocks in the solar system, fractionally crystallized iron meteorites provide insight on the early stages of planet formation. These meteorites are interpreted as fragments of cores from planetesimals that melted and subsequently differentiated due to heating by the decay of short-lived radioactive isotopes like $^{26}$Al and $^{60}$Fe (Goldstein et al., 2009; Mittlefehldt et al., 1998; Moskovitz and Gaidos, 2011). Though these meteorites are highly evolved, differences in their composition and structure provide a basis for classification (Haack and McCoy, 2005). Fourteen well-defined groups of iron meteorites have been identified, most of which are thought to represent the cores of distinct parent bodies (Goldstein et al., 2009). While the classification of these groups is generally agreed upon, details of their formation, such as parent body size, are less certain.

The origin of the group IVA iron meteorites has long been debated due to several unusual properties (Haack et al., 1996; Rasmussen et al., 1995; Ruzicka and Hutson, 2006; Scott et al., 1996; Wasson et al., 2006; Wasson and Richardson, 2001; Willis and Wasson, 1978; Yang et al., 2008). First, they display the widest range of metallographic cooling rates (100–6600 K/Myr) of any iron meteorite group (Yang et al., 2008). These rates were recorded during the formation of the Widmanstätten pattern (WP, a structure of interleaved bands of kamacite and taenite) as the core cooled from 1000 to 700 K. In addition, the diameters of cloudy zone (CZ) particles at the boundaries of taenite crystals suggest that the IVA cooling rates between 600 and 500 K varied by a factor of fifteen (Yang et al., 2007). Second, several IVAs contain silicate inclusions, which have been explained through a host of impact and melt evolution scenarios (Haack et al., 1996; McCoy et al., in press; Ruzicka and Hutson, 2006; Ulff-Møller et al., 1995; Wasson et al., 2006). Third, they are significantly depleted in moderately volatile siderophile elements relative to chondrites and other iron groups (McCoy et al., in press; Wasson and Richardson, 2001; Yang et al., 2008). Lastly, though not exclusive to the IVAs, their trace element abundances are consistent with sampling a majority of their parent core's fractional crystallization sequence (McCoy et al., in press; Ruzicka and Hutson, 2006; Scott et al., 1996; Wasson and Richardson, 2001).

One formation scenario that reasonably explains these properties (see Yang et al. (2008) and Ruzicka and Hutson (2006) for overviews of other models) suggests that the differentiated IVA parent body was

* Corresponding author.
*E-mail address:* nmoskovitz@dtm.ciw.edu (N.A. Moskovitz).

0012-821X/$ – see front matter © 2011 Elsevier B.V. All rights reserved.
doi:10.1016/j.epsl.2011.06.010

originally ~1000 km in diameter prior to a hit-and-run collision with a comparably massive proto-planet (Asphaug et al., 2006; Yang et al., 2007). This collision released a string of metal-rich fragments that eventually cooled to crystallization without the insulating effects of an overlying silicate mantle. In this scenario, the isolated core that would eventually be disrupted to produce the IVA meteorites must have been ~300 km in diameter to reproduce the wide range of metallographic cooling rates. A lack of insulating mantle is necessary to achieve rapid cooling (>1000 K/Myr) near the surface and the large size ensures that the center of the body cools slowly (~100 K/Myr).

This formation scenario merits revisiting in light of a recent U–Pb age for the IVA Muonionalusta, which indicates system closure (i.e. cooling below ~600 K) at 4565.3 ± 0.1 Ma (Blichert-Toft et al., 2010). This is the earliest measured age for any fractionally crystallized iron. It falls only ~1 Myr after the basaltic angrite Asuka 881394, the oldest differentiated rock in the Solar System (Wadhwa et al., 2009), and is less than 2.5 Myr after the formation of CAIs (calcium–aluminum-rich inclusions), generally considered to be the first solids to condense from the solar nebula. The aim of this paper is build upon the IVA formation model first presented in Yang et al. (2007) by taking into account newly available constraints on the evolution of the IVA parent core. In Section 2 we present a fractional crystallization model to provide context for the origin of Muonionalusta relative to other IVAs. In Section 3 we outline a thermal conduction model that includes heating by the decay of $^{60}$Fe. This thermal model and the result of the fractional crystallization calculation are used to constrain the size of the IVA core and make predictions for the closure ages of other IVAs (Section 4). In Section 5 we discuss the sensitivity of our results to various assumptions inherent to the thermal model. In Section 6 we summarize and discuss the broader implications of this work.

## 2. Model of IVA fractional crystallization

To estimate the extent of fractional crystallization required to produce Muonionalusta we model the IVA system assuming 3% and 0.1% initial S and P, respectively, using an approach similar to that of Walker et al. (2008) for the IVB irons (Fig. 1). Initial Re and Os concentrations of 295 and 3250 ppb, respectively, are estimated for the IVA parental melt. Details of this model are provided in McCoy et al. (in press). For these starting parameters, the Re and Os concentrations of Muonionalusta are attained after ~60% fractional crystallization, assuming that it has a composition consistent with an equilibrium solid. Appropriate concentrations are attained after 50% fractional crystallization if Muonionalusta has a composition consistent with that of the evolving IVA liquid. Mixtures of solid and liquid compositions are achieved by intermediate extents of fractional crystallization. This result is generally consistent with the model of Wasson and Richardson (2001), who generated a composition similar to Muonionalusta after ~40% and ~55% fractional crystallization, using Au versus Ir and As versus Ir plots, respectively. It is also consistent with Yang et al. (2008) who showed that an iron with 8.4% Ni-content like Muonionalusta would crystallize after ~60% solidification of a core with initial 3 wt.% S.

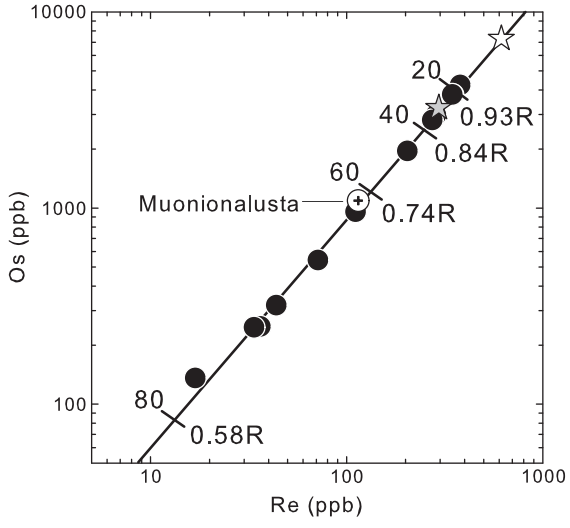


**Fig. 1.** Plot of Re versus Os (in ppb) for 14 group IVA iron meteorites. Muonionalusta is shown by the open circle with a cross. The solid line is the fractional crystallization trend for 50:50 mixes of equilibrium solids and liquids, using parameters discussed in the text. Tick marks indicate 20 through 80% extents of fractional crystallization (equivalent to 0.58–0.93R in an inwardly crystallizing metallic core). For this model, Muonionalusta is produced after ~60% fractional crystallization. The gray star represents the assumed initial liquid composition; the open star denotes the composition of the first solid to form from this liquid.

For an inwardly crystallizing core, as expected for the IVA parent (Haack and Scott, 1992; Ruzicka and Hutson, 2006; Yang et al., 2008), these data suggest that Muonionalusta formed between approximately 80–70% of the parent body radius, with 70% representing the best fit to our data (Fig. 1). This sub-surface origin is consistent with Muonionalusta's Ni abundance (an indicator of cooling rate), which is intermediate to other IVAs (Blichert-Toft et al., 2010; Yang et al., 2008).

## 3. Thermal conduction model

Because of the need for rapid cooling, our model, like that of Yang et al. (2007), begins with a body without any insulating silicate mantle. This model is based on the 1D thermal conduction equation (Moskovitz and Gaidos, 2011) and assumes a metallic sphere with the following properties: density 7500 kg/m$^3$, thermal conductivity 50 W/m/K, specific heat 400 J/kg/K, initial uniform temperature of 1750 K, and a fixed boundary temperature of 200 K. These material properties are within 20% of those used in other thermal models for differentiated bodies and are generally applicable to iron alloys (Ghosh and McSween, 1998, 1999; Hevey and Sanders, 2006; Moskovitz and Gaidos, 2011; Yang et al., 2007). The initial and boundary temperatures match those used by Yang et al. (2007). We use a fixed-temperature, Dirichlet boundary condition, which is simpler to implement than a radiative boundary condition, does not introduce significant error for the range of temperatures in which we are interested, and produces results no different from a radiative boundary for all radii up to a few km from the surface (Ghosh and McSween, 1998; Moskovitz and Gaidos, 2011; Yang et al., 2007). The boundary at 200 K is an approximation for the ambient temperature in the solar nebula (Yang et al., 2007). In Section 5.2 we show that our results are insensitive to a reasonable range of assumed initial and boundary temperatures.

One difference between our model and those of previous investigators is that we have considered heating by the decay of $^{60}$Fe. Previous models (e.g. Haack et al., 1990; Yang et al., 2008) assumed that no heat sources were available after $^{26}$Al caused melting and differentiation. However, the solar system's initial abundance of $^{60}$Fe relative to its stable isotope $^{56}$Fe is not precisely known. Therefore we present two scenarios for the IVA parent core: one in which the core thermally evolves with a maximum possible abundance of $^{60}$Fe and the second in which no $^{60}$Fe is present. These scenarios produce lower and upper limits respectively to the size of the IVA core. After accounting for a recently revised half-life of 2.62 Myr and properly reduced mass spectrometry results, a reasonable maximum for the ratio $^{60}$Fe/$^{56}$Fe at the time of CAI formation is $4\times10^{-7}$ (Mishra et al., 2010; Ogliore et al., 2011; Rugel et al., 2009; Telus et al., 2011). For the maximum heating case, we adopt this half-life and abundance, along with a decay energy of 3.04 MeV and an Fe mass fraction of 90% for the IVA parent body (Ghosh and McSween, 1998; Mittlefehldt et al., 1998). This case assumes that all of the chondritic $^{60}$Fe is sequestered into the core, again resulting in an upper limit to the energy available from radiogenic decay.

Other studies suggest that the initial $^{60}Fe/^{56}Fe$ ratio was up to several orders of magnitude lower and/or heterogeneously distributed in the solar nebula, resulting in reservoirs largely depleted in $^{60}Fe$ (Chen et al., 2009; Quitte et al., 2010; Spivak-Birndorf et al., 2011; Tang and Dauphas, 2011). To bracket the range of possible abundances we also consider the thermal evolution of the IVA parent core in the absence of any $^{60}Fe$. This minimum-$^{60}Fe$ model is analogous to that presented by Yang et al. (2008), though we now use this model to match the additional constraints of age and formation radius for Muonionalusta. The specific lower limit for $^{60}Fe$ is not critically important; once $^{60}Fe/^{56}Fe$ drops more than an order of magnitude below the upper limit, i.e. $\leq 5\times10^{-8}$, the energy available from the decay of $^{60}Fe$ would have been insignificant in the overall thermal budget of the IVA parent body.

The thermal model assumes that the IVA core was fully formed at 4567.7, a weighted mean of recently measured CAI ages (Burkhardt et al., 2008; Jacobsen et al., 2008). The statistical uncertainty on this weighted mean is 0.3 Myr, though systematic errors could be as large as 1 Myr (see Section 5.4, Amelin et al., 2010). This assumption requires that accretion, differentiation and exposing of the IVA core occurred much faster than the $\sim10^6$-year timescales for $^{60}Fe$ heating and conductive cooling (Moskovitz and Gaidos, 2011; Rugel et al., 2009). This is consistent with hydrodynamic simulations of planetesimal formation in turbulent proto-planetary disks that show bodies as large as 1000 km accreted in much less than $10^3$ years (Johansen et al., 2007). In Section 5.5 we show that this nearly instantaneous accretion anytime within 1.5 Myr of CAI formation, a limit for fractionally crystallized iron cores, does not affect our size estimates for the IVA core (Haack and McCoy, 2005; Qin et al., 2008). The assumed initial temperature of 1750 K at 4567.7 Ma is unphysical, however a variety of heat sources (e.g. $^{26}Al$ decay and impacts) could have contributed to the global heating of bodies hundreds of km in size (Keil et al., 1997; Moskovitz and Gaidos, 2011). These heat sources would have been relevant on timescales of $10^5-10^6$ years.

## 4. Models of the IVA core

Fig. 2 shows how temperature varies as a function of cooling rate in two different exposed cores. These temperature profiles are shown for a range of depths, from the center of the body up to 97% of the radius $R$. The top panel (A) depicts a case with maximum $^{60}Fe/^{56}Fe = 4\times10^{-7}$ and $R = 50$ km; the bottom panel (B) depicts a core with no $^{60}Fe$ and $R = 130$ km.

The release of energy from the decay of $^{60}Fe$ prolongs cooling and reduces cooling rates. Thus, the body in Fig. 2A, which is only 50 km in radius, exhibits cooling rates as small as 140 K/Myr at its center during the formation of the Widmanstätten pattern (1000–700 K) and a range of rates during the formation of cloudy zone particles (600–500 K) that is consistent with measurements. Furthermore, WP cooling rates at 0.7R are as expected for Muonionalusta based on rates measured for its compositional analog Seneca Township (300–1200 K/Myr, Yang et al., 2008). If no $^{60}Fe$ were present on a body this small then none of these constraints would be met: the lowest cooling rates during WP formation would be an order of magnitude larger, the CZ rates would only vary by a factor of 10, and the WP cooling rates at 0.7R would be larger than those measured for Seneca Township. Smaller bodies with this $^{60}Fe$ abundance cool too quickly to reproduce the low end of the IVA range of WP rates. As such, a radius of 50 km is a lower limit for a core to be able to reproduce the IVA cooling rate data.

An upper limit for the size of the IVA core is depicted in Fig. 2B. In this case, no $^{60}Fe$ is present, thus requiring $R = 130$ km to achieve slow cooling (~100 K/Myr) near the center. A body with these properties meets the WP, CZ and Seneca cooling rate constraints. Although a larger body would produce the necessary range of WP and CZ rates, the cooling rates at 0.7R would be too slow (<300 K/Myr) for Seneca Township.

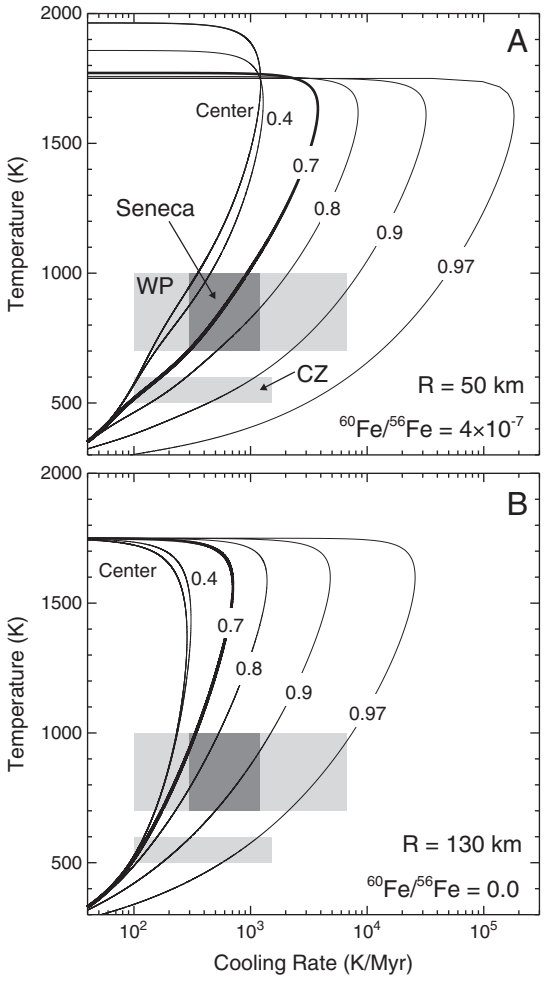


**Fig. 2.** Cooling rate versus temperature at different depths, expressed as fractions of the parent radius, in exposed cores with maximal $^{60}Fe$ (A) and in the absence of $^{60}Fe$ (B). The light gray regions represent temperatures and measured IVA cooling rates during formation of the Widmanstätten pattern (WP) and cloudy zone particles (CZ). The dark gray box represents the measured cooling rates for Seneca Township, a sample with similar Ni-content to Muonionalusta. In each case the sizes of the cores have been adjusted such that the measured ranges of WP and CZ rates are reproduced, and so that a radius of 0.7R crystallizes at the rates measured for Seneca. These two examples represent upper (R = 130 km) and lower (R = 50 km) limits to the size of the IVA core.

Therefore, the cooling rates modeled in Fig. 2 bracket the size of the IVA core to somewhere between 50 and 130 km.

The age of Muonionalusta further constrains the size of the IVA core. Fig. 3 shows the times at which different depths in exposed cores reach U–Pb isotopic closure at 600 K (Blichert-Toft et al., 2010). The two panels again correspond to $^{60}Fe/^{56}Fe = 4\times10^{-7}$ (A) and $^{60}Fe/^{56}Fe = 0$ (B) and produce lower and upper size limits respectively. For the former, Muonionalusta would crystallize at 4565.3 Myr in a core with a radius of 55 km (i.e. where the bold curve intersects the shaded region). For the later, the age of Muonionalusta is reproduced for a core 110 km in radius.

Matching both the cooling rates (Fig. 2) and the U–Pb age at the expected depth of Muonionalusta's origin (Fig. 3) suggests that the IVA core was between 50 and 110 km in radius, depending upon the assumed initial abundance of $^{60}Fe$. Below this lower limit the entire body would reach U–Pb closure within 2.5 Myr (Fig. 3A), requiring that Muonionalusta come from the center of the IVA core. This would unreasonably preclude cooling rates slower than the 500 K/Myr inferred for Muonionalusta (Blichert-Toft et al., 2010). Conversely, a core with R>110 km would not reach U–Pb closure in <2.5 Myr at 0.7R (Fig. 3B). We adopt R = 50 km as a lower limit rather than 55 km because several of the assumptions in these models hasten cooling

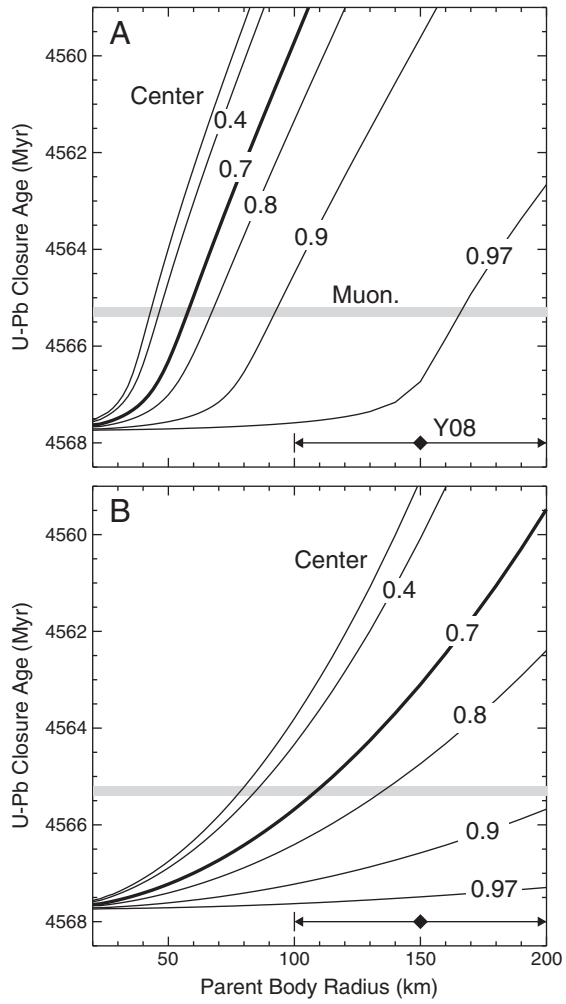


**Fig. 3.** U–Pb closure ages at different depths for a range of parent body sizes with initial $^{60}Fe/^{56}Fe = 4\times10^{-7}$ (panel A) and $^{60}Fe/^{56}Fe = 0$ (panel B). The thick curve (0.7R) represents the expected radius of Muonionalusta's origin. The gray region denotes Muonionalusta's closure age of 4565.3 ± 0.1 Ma. The size estimate for the IVA parent body from Yang et al. (2008) is shown at the bottom right. The closure age at the formation radius of Muonionalusta is reproduced for core radii between 50 (panel A) and 110 km (panel B), depending upon the initial abundance of $^{60}Fe$.

and thus demand an increase in size to produce cooling rates ~100 K/My (see Section 5).

In these models, size and $^{60}Fe$ abundance are degenerate properties whose variation produces a series of solutions that fulfill the cooling rate and age constraints. The examples in Figs. 2 and 3 are end-member cases that bracket the range of possibilities. If the initial $^{60}Fe$ abundance in the IVA parent core were known, then it is possible to predict a specific relationship between U–Pb closure age and cooling rate. For example, a given depth profile in Fig. 2 records a range of cooling rates between 1000 and 700 K and a U–Pb closure age at 600 K. Table 1 presents predicted ages for several IVAs by assuming that the mean cooling rate measured for each sample corresponds to the rate midway between 1000 and 700 K. These predictions are specific to the case of R = 50 km and $^{60}Fe/^{56}Fe = 4\times10^{-7}$ and are simply intended to highlight several implications of this formation model.

First, the results in Table 1 predict a wide range of U–Pb closure ages from 4564.0 to 4567.5 Ma. This range of several Myr is a general outcome of these models, irrespective of the assumed $^{60}Fe$ abundance, and is resolvable with the current precision of U–Pb dating techniques (Blichert-Toft et al., 2010). None of our models produce rates less than ~140 K/Myr and thus cannot predict the closure ages of the four most chemically evolved IVAs (Duchesne, Chinautla, New Westville and Steinbach), though it is likely they reached U–Pb closure after 4654 Ma. We do not view this as a significant failure of the model considering the large uncertainties and many assumptions that have been made (see Section 5). Varying input parameters such at the specific heat could reduce the calculated cooling rates to the 100 K/My that is measured for Duchesne.

**Table 1**
Cooling rates and U–Pb closures ages for a IVA core with R = 50 km and $^{60}Fe/^{56}Fe = 4\times10^{-7}$.

| Meteorite | Cooling rate[a] (K/Myr) | Predicted U–Pb closure age (Ma) |
|---|---|---|
| La Grange | 6600 | 4567.5 |
| Obernkirchen | 2900 | 4567.4 |
| Bishop Canyon | 2500 | 4567.4 |
| Jamestown | 1900 | 4567.3 |
| Gibeon | 1500 | 4567.2 |
| Seneca Township | 580 | 4566.4 |
| Altonah | 420 | 4565.8 |
| Muonionalusta | 290-940[b] | 4565.3 ± 0.1[c] |
| Bushman Land | 260 | 4564.5 |
| Duel Hill | 220 | 4564.0 |
| Steinbach | 150 | <4564 |
| New Westville | 120 | <4564 |
| Chinautla | 110 | <4564 |
| Duchesne | 100 | <4564 |

[a] Yang et al. (2008).
[b] Model prediction.
[c] Blichert-Toft et al. (2010).

Second, the correlation between closure age and cooling history predicts cooling rates for Muonionalusta. For example, when R = 50 km and $^{60}Fe/^{56}Fe = 4\times10^{-7}$, Muonionalusta's closure age suggests cooling rates between 290 and 940 K/Myr, which by design are similar to the range of rates for Seneca Township (Yang et al., 2008).

Lastly, this formation model predicts that IVAs with the fastest cooling rates will have the oldest U–Pb closure ages. In the example shown in Table 1, the predicted ages for samples like La Grange and Bishop Canyon are only a few hundred thousand years separated from the formation of CAIs. If this formation scenario is correct, then these IVAs may represent the oldest differentiated rocks in the Solar System.

## 5. Assumptions in the thermal model

### 5.1. Neglected processes

The release of latent heat during crystallization, the temperature dependence of specific heat, and the effect of an insulating layer have been neglected in these models. The net latent heat available in the Fe–Ni–S system is 270 kJ/kg (Haack et al., 1990), which is less than the total energy released by the decay of $^{60}Fe$ when the initial $^{60}Fe/^{56}Fe > 6\times10^{-8}$. Unfortunately this critical $^{60}Fe$ abundance is intermediate in the range of current best estimates (Chen et al., 2009; Mishra et al., 2010; Quitte et al., 2010; Telus et al., 2011; Spivak-Birndorf et al., 2011; Tang and Dauphas, 2011). As such, it is difficult to determine the relative importance of latent heat release without a well-constrained $^{60}Fe$ abundance. Nevertheless, a release of 270 kJ/kg of latent heat could increase temperatures by up to several hundred Kelvin (assuming no conductive loss of heat and a heat capacity of 400 J/kg/K) and, like any additional heat source, would prolong cooling. For all models presented here, the temperature-independent specific heat is near the lower limit for metallic iron and thus hastens cooling (Ghosh and McSween, 1999).

To quantify the effects of an insulating mantle we have run a series of simulations for an R = 50-km body with $^{60}Fe/^{56}Fe = 4\times10^{-7}$ and a surface layer with low thermal diffusivity. These calculations suggest that a silicate mantle (thermal conductivity = 2 W/m/K, heat capacity = 1200 J/kg/K) thicker than ~0.5 km would prevent rapid cooling

>1000 K/Myr for nearly all radii. With an initially chondritic composition, the core should be of order 40% of the radius (Haack et al., 1990). Therefore, any reasonable thickness for a silicate mantle would prevent the rapid cooling rates (>1000 K/Myr) measured for some IVAs. This argues strongly in favor of a collision exposing the IVA core before it cooled below 1000 K (Yang et al., 2007).

We have performed a similar calculation for a surface regolith (thermal conductivity = 0.01 W/m/K, heat capacity = 1200 J/kg/K) in place of a mantle (Haack et al., 1990). A regolith thicker than ~50 m would reduce the range of cooling rates to below that measured for the IVAs. For the range of regolith and mantle thickness considered, 0–0.5 km and 0–5 km respectively, the dominant effect on the thermal evolution is a reduction of the highest cooling rates at the base of the insulating layer. These insulating layers do not influence central cooling rates until they become sufficiently thick (approximately 0.5 km and 5 km respectively) such that the timescale over which they conductively transfer heat becomes comparable to the timescale of conductive heat loss across the whole of the 50-km metallic core.

Neglecting the release of latent heat, the temperature dependence of specific heat, and the effect of an insulating layer, act to hasten the loss of thermal energy and thus artificially increase interior cooling rates. Since the slowest IVA cooling rates are most difficult to reproduce in a mantle-free body, treatment of these phenomena could extend the estimated range of possible parent bodies to sizes less than R = 50 km.

Our model does not treat the convection of molten material, which would occur for melt fractions >50%. For the Fe–Ni–S system, the assumed initial temperature of 1750 K would correspond to high degrees of partial melting. The details of convective processes in an exposed molten core are not well understood and are beyond the scope of this study. Convection in such a system would increase the rate of heat loss from the interior and perhaps require larger bodies to ensure ~100 K/Myr cooling near the center.

### 5.2. Initial and boundary temperatures

The ability of our model to reproduce the IVA cooling rates is unaffected by changes to initial temperatures down to 1000 K and nebular temperatures up to 300 K. For instance, the range of cooling rates during the formation of the Widmanstätten pattern (1000–700 K) from the center to 0.9R for the R = 50 km body in Fig. 2A is 140–8500 K/Myr. Reducing the initial temperature of this body from 1750 K to 1000 K changes this range to 140–16,000 K/Myr, only the fastest cooling rates near the surface are affected. The reason for the increase in cooling rates at the upper end of this range is due to our focus on the narrow range of temperatures at which the Widmanstätten pattern forms. In other words, the lowering of initial temperature shifts the curves in Fig. 2 downwards, which causes a wider range of rates between 1000 and 700 K. Increasing the boundary temperature up to a plausible maximum of 300 K (Yang et al., 2007) also has little effect on cooling rates and results in a range of 110–6500 K/Myr for the above example. The thermal model of Yang et al. (2008) is similarly insensitive to changes in initial and boundary temperatures.

### 5.3. U–Pb closure temperature

These models assume a U–Pb closure temperature of 600 K, however this value is not well constrained. Blichert-Toft et al. (2010) suggest 573 K based on the assumption that the closure temperature of Pb in sulfides is the same as that of Os. Studies of U and Pb diffusion in silicates suggest closure temperatures of about 625 ± 50 K (Spear and Parrish, 1996). This suggests that our adopted closure temperature of 600 K may be accurate to approximately ±100 K, but specific measurements of U/Pb diffusion in sulfides at elevated temperatures are essential for interpreting the U–Pb ages of iron meteorites. This uncertainty predominantly affects the calculated closure ages in Fig. 3. For example, a lower closure temperature of 500 K demands a slightly smaller body (approximately 50 km rather than 55 km when $^{60}Fe/^{56}Fe = 4\times10^{-7}$) to match the age constraint for Muonionalusta. This difference is insignificant relative to other uncertainties in the model.

### 5.4. Precision of U–Pb ages

We have assumed that the closure age of Muonionalusta is 4565.3 ± 0.1 Ma (Blichert-Toft et al., 2010). However, this value could be in error by ~1 Myr due to variations in the $^{238}U/^{235}U$ value of CAIs (Amelin et al., 2010). Ages younger by 1 Myr would permit larger parent bodies because of the additional time available to reach U–Pb closure. Older ages would require smaller bodies such that closure occurs even faster. Therefore, this uncertainty translates into a slightly broader range of acceptable parent body sizes. At the lower size limit this effect is insignificant, i.e. less than 5 km difference from our standard assumption of CAI ages equal to 4567.7 Ma. At the upper limit, a younger closure age for Muonionalusta could allow parent bodies up to R = 125 km.

### 5.5. Effect of delayed accretion

Hf–W chronometry and thermal modeling suggest that fractionally crystallized iron meteorite parent bodies accreted within 1.5 Myr of CAI formation (Qin et al., 2008). We adopt this constraint as an upper limit to the time of formation and use it to recalculate the results in Figs. 2 and 3. For Fig. 2A, the range of cooling rates for radii inside of 0.9R are 140–8500 K/Myr. Delaying accretion to 1.5 Myr has little effect on these rates, it simply reduces the amount of live $^{60}Fe$ and produces a range of cooling rates from 225 to 9000 K/Myr. Fig. 2B is unaffected by the assumed time of accretion due to a lack of $^{60}Fe$. In short, later times of accretion primarily act to dampen peak temperatures and have little influence on cooling rates below 1000 K.

The size constraints for the IVA core are similarly unaffected by times of accretion up to 1.5 Myr. Delayed accretion effectively shifts the curves in Fig. 3 upwards, and does not affect our upper limit for the core size. In other words, the point of intersection of the 0.7R curve and the age of Muonionalusta will never shift to larger radii with later times of accretion. Delayed accretion also has little effect on the lower size limit. This insensitivity is a result of competing processes in cores heated by $^{60}Fe$. With delayed accretion less time is available to reach U–Pb closure, thus requiring faster cooling to produce Muonionalusta at 0.7R. But, less live $^{60}Fe$ is present to prolong cooling. These two effects act to cancel out one another.

## 6. Conclusions

We have argued that the parent core of the iron IVA meteorites was between 50 and 110 km in radius, dependent primarily on the abundance of live $^{60}Fe$ incorporated into the core. Cores in this size range follow a crystallization sequence that match constraints set by metallographic cooling rates (Yang et al., 2007, 2008), a U–Pb age (Blichert-Toft et al., 2010) and geochemical data (McCoy et al., in press; Rasmussen et al., 1995; Ruzicka and Hutson, 2006; Wasson and Richardson, 2001). An estimate of R = 150 ± 50 km by Yang et al. (2008) is consistent with the upper end of this size range, though our models are also consistent with a IVA core up to three times smaller. The lower gravity in a smaller parent may facilitate the trapping of silicate inclusions in a molten core (Ruzicka and Hutson, 2006). The probability of near-catastrophic collisions necessary to expose a molten core should be greater for smaller bodies (Bottke et al., 2005). The dependence of our results on a single old age emphasizes the need for additional dating of Muonionalusta and other IVAs. Experimental confirmation of Muonionalusta's predicted cooling rates of ~500 K/Myr is

equally important to future studies on the thermal evolution of the IVA core.

The range of cooling rates for the IVAs is the greatest of any chemical group (Haack and McCoy, 2005; Yang and Goldstein, 2006; Goldstein et al., 2009; Yang et al., 2010), suggesting they represent one of the largest iron meteorite parent cores with measured rates. Determination of cooling rates for currently unmeasured groups could reveal otherwise. With a radius between 50 and 110 km, the IVA core must have derived from a fully differentiated parent body that was at least twice as large (Haack et al., 1990). However, due to large uncertainties regarding the hit-and-run formation scenario, it is difficult to precisely estimate the size of the fully differentiated IVA parent body prior to the collision. Nevertheless, our results suggest that planetary bodies ~200–500 km in diameter were present during the first few Myr of solar system history, with a possibility of even larger bodies depending upon the details of the collision that exposed the IVA core and the currently unknown cooling rates of other iron groups. This removes the necessity, though does not preclude the possibility of $10^3$ km, proto-planetary bodies early in solar system history (Yang et al., 2008).

For this scenario of formation within an exposed core, IVAs with fast cooling rates (>1000 K/Myr) may have absolute ages separated by as little as a few times $10^5$ years from CAI formation (Table 1). Confirmation of this would provide important clues to understanding the timescales involved in the formation of the first planetary bodies in the solar system.

Though Muonionalusta experienced shock melting, one of its troilite grains somehow preserved the old age measured by Blichert-Toft et al. (2010). If similar troilite grains can be dated in other IVAs, then the resulting range of U–Pb closure ages will provide a tighter constraint on the size of the IVA parent. For example, the range of closure ages for an R = 50-km core is less than half that of an R = 100-km core (Fig. 3). The core sizes of other fractionally crystallized iron groups with diverse cooling rates, such as the IIAB, IIIAB and IVBs (Yang et al., 2008, 2010), can be constrained by modeling both cooling rates and U–Pb ages, assuming such ages can be measured.

Previous studies on the formation and crystallization of fractionally crystallized irons assumed that the thermal effects of $^{60}$Fe were insignificant. This is reasonable for irons that formed inside of cores surrounded by insulating mantles since they would crystallize after $^{60}$Fe was largely extinct. However, the age of Muonionalusta suggests that mantle-free cores may have crystallized when $^{60}$Fe was still extant. As we have shown, cooling rates can be affected by the decay of this isotope. Unfortunately, current uncertainties in its initial abundance make it difficult to specifically quantify the relevance of $^{60}$Fe decay to the thermal evolution of these parent bodies. If $^{60}$Fe was present during the crystallization of iron groups like the IVA, IIAB, IIIAB and IVBs, then updated models will result in a reduction of the inferred sizes of these parent bodies.

## Acknowledgements

We thank Eric Gaidos and Rick Carlson for helpful comments regarding this study. Ed Scott, Joe Goldstein and an anonymous referee provided thoughtful reviews that led to significant improvement of this manuscript. NAM acknowledges support from the Carnegie Institution of Washington and the NASA Astrobiology Institute. This work was in part supported by NASA Cosmochemistry grant NNX10AG94G to RJW.

## References

Amelin, Y., Kaltenbach, A., Iizuka, T., Stirling, C.H., Ireland, T.R., Pataev, M., Jacobsen, S., 2010. U–Pb chronology of the Solar System's oldest solids with variable $^{238}$U/$^{235}$U. Earth Planet. Sci. Lett. 300, 343–350.

Asphaug, E., Agnor, C.B., Williams, Q., 2006. Hit-and-run planetary collisions. Nature 439, 155–160.

Blichert-Toft, J., Moynier, F., Lee, C.A., Telouk, P., Albarede, F., 2010. The early formation of the IVA iron meteorite parent body. Earth Planet. Sci. Lett. 296, 469–480.

Bottke, W.F., Durda, D.D., Nesvorny, D., Jedicke, R., Morbidelli, A., Vokrouhlicky, D., Levison, H.F., 2005. Linking the collisional history of the main asteroid belt to its dynamical excitation and depletion. Icarus 179, 63–94.

Burkhardt, C., Kleine, T., Bourdon, B., Palme, H., Zipfel, J., Friedrich, J.M., Ebel, D.S., 2008. Hf–W mineral isochron for Ca, Al-rich inclusions: age of the solar system and the timing of core formation in planetesimals. Geochim. Cosmochim. Acta 72, 6177–6197.

Chen, J.H., Papanastassiou, D.A., Wasserburg, G.J., 2009. A search for nickel isotopic anomalies in iron meteorites and chondrites. Geochim. Cosmochim. Acta 73, 1461–1471.

Ghosh, A., McSween, H.Y., 1998. A thermal model for the differentiation of asteroid 4 Vesta based on radiogenic heating. Icarus 134, 187–206.

Ghosh, A., McSween, H.Y., 1999. Temperature dependence of specific heat capacity and its effect on asteroid thermal models. Meteorit. Planet. Sci. 34, 121–127.

Goldstein, J.I., Scott, E.R.D., Chabot, N.L., 2009. Iron meteorites: crystallization, thermal history, parent bodies and origin. Chem. Erde 69, 293–325.

Haack, H., McCoy, T.J., 2005. Iron and stony-iron meteorites. In: Holland, H.D., Turekian, K.K. (Eds.), Meteorites, Comets and Planets, Treatise on Geochemistry, 1. Elsevier-Pergamon, Oxford, pp. 325–347.

Haack, H., Scott, E.R.D., 1992. Asteroid core crystallization by inward dendritic growth. J. Geophys. Res. 97, 14727–14734.

Haack, H., Rasmussen, K.L., Warren, P.H., 1990. Effects of regolith/megaregolith insulation on the cooling histories of differentiated asteroids. J. Geophys. Res. 95, 5111–5124.

Haack, H., Scott, E.R.D., Love, S.G., Brearley, A.J., McCoy, T.J., 1996. Thermal histories of IVA stony-iron and iron meteorites: evidence for asteroid fragmentation and reaccretion. Geochim. Cosmochim. Acta 60, 3103–3113.

Hevey, P.J., Sanders, I.S., 2006. A model for planetesimal meltdown by $^{26}$Al and its implications for meteorite parent bodies. Meteorit. Planet. Sci. 41, 95–106.

Jacobsen, B., Yin, Q., Moynier, F., Amelin, Y., Krot, A.N., Nagashima, K., Hutcheon, I.D., Palme, H., 2008. $^{26}$Al–$^{26}$Mg and $^{207}$Pb–$^{206}$Pb systematics of Allende CAIs: canonical solar initial $^{26}$Al/$^{27}$ Al reinstated. Earth Planet. Sci. Lett. 272, 353–364.

Johansen, A., Oishi, J.S., Mac Low, M., Klahr, H., Henning, T., Youdin, A., 2007. Rapid planetesimal formation in turbulent circumstellar disks. Nature 448, 1022–1025.

Keil, K., Stoffler, D., Love, S.G., Scott, E.R.D., 1997. Constraints on the role of impact heating and melting in asteroids. Meteorit. Planet. Sci. 32, 349–363.

McCoy, T.J., Walker, R.J., Goldstein, J.I., Yang, J., McDonough, W.F., Rumble, D., Chabot, N.L., Ash, R.D., Corrigan, C.M., Michael, J.R., Kotula, P.G., in press. Group IVA irons: new constraints on the crystallization and cooling history of an asteroidal core with a complex history. Geochim. Cosmochim. Acta.

Mishra, R.K., Goswami, J.N., Tachibana, S., Huss, G.R., Rudraswami, N.G., 2010. $^{60}$Fe and $^{26}$Al in chondrules from unequilibrated chondrites: implications for early solar system processes. Astrophys. J. Lett. 714, L217–L221.

Mittlefehldt, D.W., McCoy, T.J., Goodrich, C.A., Kracher, A., 1998. Non-chondritic meteorites from asteroidal bodies. In: Papike, J.J. (Ed.), Planetary Materials, Reviews in Mineralogy, 36. Mineralogical Society of America, Washington. ch. 4.

Moskovitz, N.M., Gaidos, E., 2011. Differentiation of planetesimals and the thermal consequences of melt migration. Meteorit. Planet. Sci. 46, 903–918.

Ogliore, R.C., Huss, G.R., Nagashima, K., 2011. The problem of bias in mass spectrometry ratio estimation (abstract #1592). 42nd Lunar and Planetary Science Conference. CD-ROM.

Qin, L., Dauphas, N., Wadhwa, M., Masarik, J., Janney, P.E. Rapid accretion and differentiation of iron meteorite parent bodies inferred from 182Hf–182 W chronometry and thermal modeling. Earth Planet. Sci. Lett. 273, 94–104.

Quitte, G., Markowski, A., Latkoczy, C., Gabriel, A., Pack, A., 2010. Iron-60 heterogeneity and incomplete mixing in the early Solar System. Astrophys. J. 720, 1215–1224.

Rasmussen, K.L., Ulff-Moller, F., Haack, H., 1995. The thermal evolution of IVA iron meteorites: evidence from metallographic cooling rates. Geochim. Cosmochim. Acta 59, 3049–3059.

Rugel, G., Faestermann, T., Knie, K., Korschinek, G., Poutivtsev, M., Schumann, D., Kivel, N., Gunther-Leopold, I., Weinreich, R., Wohlmuther, M., 2009. New measurements of the $^{60}$Fe half-life. Phys. Rev. Lett. 103, 072502.

Ruzicka, A., Hutson, M., 2006. Differentiation and evolution of the IVA meteorite parent body: clues from pyroxene geochemistry in the Steinbach stony-iron meteorite. Meteorit. Planet. Sci. 41, 1959–1987.

Scott, E.R.D., Haack, H., McCoy, T.J., 1996. Core crystallization and silicate-metal mixing in the parent body of the IVA iron and stony-iron meteorites. Geochim. Cosmochim. Acta 74, 1615–1631.

Spear, F.S., Parrish, R.R., 1996. Petrology and cooling rates of the Valhalla Complex, British Columbia. Can. J. Petrol. 37, 733–765.

Spivak-Birndorf, L.J., Wadhwa, M., Janney, P.E., 2011. $^{60}$Fe–$^{60}$Ni chronology of the D-Orbigny angrite: implications for the initial Solar System abundance of $^{60}$Fe (abstract #2281). 42nd Lunar and Planetary Science Conference. CD-ROM.

Tang, H., Dauphas, N., 2011. Constraints from chondrites on the initial $^{60}$Fe/$^{56}$Fe ratio of the Solar System (abstract #1068). 42nd Lunar and Planetary Science Conference. CD-ROM.

Telus, M., Huss, G.R., Nagashima, K., Ogliore, R.C., Tachibana, S., Jilly, C.E., 2011. Possible heterogeneity of $^{60}$Fe in chondrules from primitive ordinary chondrites (abstract #2559). 42nd Lunar and Planetary Science Conference. CD-ROM.

Ulff-Møller, F., Rasmussen, K.L., Prinz, M., Palme, H., Spettel, B., Kallemeyn, G.W., 1995. Magmatic activity on the IVA parent body: evidence from silicate-bearing iron meteorites. Geochim. Cosmochim. Acta 59, 4713–4728.

Wadhwa, M., Amelin, Y., Bogdanovski, O., Shukolyukov, A., Lugmair, G.W., Janney, P., 2009. Ancient relative and absolute ages for a basaltic meteorite: implications for timescales of planetisimal accretion and differentiation. Geochim. Cosmochim. Acta 73, 5189–5201.

Walker, R.J., McDonough, W.F., Honesto, J., Chabot, N.L., McCoy, T.J., Ash, R.D., Bellucci, J.J., 2008. Modeling fractional crystallization of group IVB iron meteorites. Geochim. Cosmochim. Acta 72, 2198–2216.
Wasson, J.T., Richardson, J.W., 2001. Fractionation trends among IVA iron meteorites: contrasts with IIIAB trends. Geochim. Cosmochim. Acta 65, 951–970.
Wasson, J.T., Matsunami, Y., Rubin, A.E., 2006. Silica and pyroxene in IVA irons; possible formation of the IVA magma by impact melting and reduction of L-LL-chondrite materials followed by crystallization and cooling. Geochim. Cosmochim. Acta 70, 3149–3172.
Willis, J., Wasson, J.T., 1978. Cooling rates of group IVA iron meteorites. Earth Planet. Sci. Lett. 40, 141–150.
Yang, J., Goldstein, J.I., 2006. Metallographic cooling rates of the IIIAB iron meteorites. Geochim. Cosmochim. Acta 70, 3197–3215.
Yang, J., Goldstein, J.I., Scott, E.R.D., 2007. Iron meteorite evidence for early formation and catastrophic disruption of protoplanets. Nature 446, 888–891.
Yang, J., Goldstein, J.I., Scott, E.R.D., 2008. Metallographic cooling rates and origin of IVA iron meteorites. Geochim. Cosmochim. Acta 72, 3043–3061.
Yang, J., Goldstein, J.I., Michael, J.R., Kotula, P.G., Scott, E.R.D., 2010. Thermal history and origin of the IVB iron meteorites and their parent body. Geochim. Cosmochim. Acta 74, 4493–4506.